



WRIS.TEQ: multi-mineralic water–rock interaction, mass-transfer and textural dynamics simulator

Anthony J. Park*, Peter J. Ortoleva

Laboratory for Computational Geodynamics, Indiana University, Bloomington, IN, USA

Received 15 February 2002; received in revised form 1 June 2002; accepted 24 September 2002

Abstract

Water–rock interactions in sediments are driven by the state of disequilibrium that persists among solids and solutes due to changing temperature and stress conditions, and advective and diffusive influx and efflux of solutes. Water–rock interactions bring about changes to sediment composition and texture through a complex chemical reaction network. These reactions can be divided into two types: solid–solute and solute–solute.

Reactions of solids and solute are kinetic, i.e., they depend on compositions of solids and water, temperature, pore water pressure, and stress. Speciation among solutes are described by thermodynamic relations that depend on water composition and temperature. Both reaction mechanisms, mediated by pore water, are strongly interdependent.

WRIS.TEQ is a comprehensive Reaction–Transport–Mechanical (RTM) simulator that accounts for multi-mineralic water–rock interaction mechanisms of kinetics and thermodynamics, and mass transfer due to advection and diffusion. Moreover, the simulator's dynamic compositional and textural model based on a composite-media approach allows self-consistent evolution of sediment composition and texture due to water–rock interactions. Thus, the program can be used to make reliable predictions of sediment alteration due to water–rock interactions at the level it was previously not possible.

This article describes the fundamentals of water–rock interaction and composite medium models used in the simulator WRIS.TEQ, and how the program is constructed. The utility of the program is demonstrated by simulated diagenetic alteration of sediments composed of complex mineralogy and heterogeneity.

© 2003 Elsevier Science Ltd. All rights reserved.

Keywords: Diagenesis; Kinetic and thermodynamic reactions; Diffusive and advective mass-transfer; Process-oriented model; Reaction–transport–mechanical (RTM) simulator

1. Introduction

Chemical interactions between solids and water in sediments are driven by chemical disequilibrium persisting in the system. The cause of the disequilibrium may be from chemically unstable assemblages of solids that are mediated by water. Unstable solid assemblages occur when different solids—minerals and organic materials—share common constituents but possess different chemical and thermodynamic properties. Thus, water–rock

interactions occurring in sediments are natural tendencies of solid–water assemblages to achieve equilibrium.

However, several factors make it difficult for many geologic systems to reach equilibrium. These factors include constantly changing thermal and stress conditions; slow reaction rates of minerals; influx and efflux of solutes; and diffusive migration of solutes. Furthermore, the progression of water–rock interaction itself has the tendency to change the reactivity properties of sediments by altering their compositions and texture.

In this paper we focus on how multiple reacting minerals can be accounted for in a basin or hydrologic model. Whereas there are other models that attempt to

*Corresponding author.

E-mail address: park2@indiana.edu (A.J. Park).

account for chemical interactions involving multiple solid species, the model presented here differs in two aspects: (1) Reactions among solids and solutes are described using fully coupled kinetic rate law and thermodynamic descriptions; (2) Sediment is described using a composite media model that accounts for textural dynamics. Thus, the model can predict and simulate the affects of mineralogical changes taking place in sediment, and the associated changes in the sediment properties, such as porosity, reactive surface area, permeability, etc.

The water–rock interaction processes outlined previously have been implemented as modules in chemical interaction of rock and fluid (CIRF.B) simulator of Laboratory for Computational Geodynamics, Indiana University (Ortoleva, 1994). CIRF.B is a Reaction–Transport–Mechanical (RTM) simulation platform that hosts a number of phenomenology-based modules, such as hydrology, rheology, organic maturation and fracturing, to name a few. This modular structure of CIRF.B allows its reconfiguration to yield problem-specific simulators. Thus, the Water–rock Interaction in sediment: texture evolution and quality (WRIS.TEQ) simulator is a specific configuration of CIRF.B that utilizes its framework (1) to manage the simulation-domain configuration, (2) for geological, physical and chemical data management, and (3) to link with a hydrologic module to assess fluid flow. To construct WRIS.TEQ, the water–rock interaction module (WRI) module was integrated into the flow of computation in CIRF.B to capture the nonlinearity that arises from the coupling of water–rock interactions, texture dynamics, and fluid flow.

2. Background and comparison with other water–rock interaction models

In recent years significant progress has been achieved toward quantitatively modeling water–rock interaction processes. Thus, sophisticated models can achieve useful results and important insights on the extent of water flow through porous and/or fractured media, and speciation of solutes in pore water at various conditions. These models fall into three categories: (1) chemical equilibrium speciation (Wolery et al., 1990; Perkins et al., 1988; Parkhurst et al., 1990), (2) reaction-path studies (White and Chuma, 1986), or (3) kinetic and continuum-based models. (Boudreau, 1996; Chen et al., 1990; Steefel and Lichtner, 1998; Steefel and Lasaga, 1994).

The function of speciation models is to compute solute species concentrations and mineral saturations using a multi-mineral, multi-solute reaction network. Speciation of solutes is calculated using a combination of solute–solute and solute–mineral reactions written in

mass-action expressions. These equations are supplemented by either mass- or charge-balance expressions (Garrels and Christ, 1990) to construct a sufficient number of equations.

Continuum-based models are developed to enhance the speciation models to account for mass transfer due to advection and diffusion/dispersion. This is achieved by solving a continuity (or conservation) equation in the form of a second-order differential equation (deGroot and Mazur, 1962) that describes zeroth-order (chemical reaction), first-order (advection) and second-order (diffusion/dispersion) behaviors of solutes. Mass transfer-reaction coupled models solve continuity equations written in non-steady-state forms (evolutionary equation; Ortoleva, 1994), and by solving the time-difference form of the equation using implicit or explicit numerical methods (Chen et al., 1990; Steefel and Lasaga, 1994; Boudreau, 1996). Other flow-speciation coupled models, such as reaction-path (White and Chuma, 1986), transition state (Lichtner, 1985), or chromatographic/reaction front models (Schechter et al., 1987) are not necessarily locally consistent with the formulation of continuity equations. However, they offer alternative methods for simulating water–rock interaction and mass transfer in porous media.

The most significant difference between WRIS.TEQ and other water–rock interaction models is the coupling of water–rock interaction and mass-transfer with sediment texture and composition evolution. Most other models assume the medium to either maintain constant porosity and permeability, or they calculate porosity change based on an empirical compaction curve. By contrast, WRIS.TEQ accounts for porosity and textural modification due to water–rock interaction by using a composite-medium approach to sediment description, whereby a sediment is described as consisting of a number of minerals, each of which is further described with geometric variables. Evolving permeability is computed using a modified Kozeny–Karman equation that utilizes the composite medium properties, which is then used by the flow solver to compute a self-consistent flow regime.

In the following sections features accounted for in WRIS.TEQ and a brief outline of the modular structure of CIRF.B are presented. Numerical methods used in WRIS.TEQ are also documented; the methods utilized in the hydrologic and other CIRF.B modules are discussed elsewhere (Tuncay et al., 2000a,b). To demonstrate the capabilities of the program, three simulations are presented: A one-element batch-type system for demonstrating the importance of compositional disequilibrium; a multi-element, heterogeneous one-dimensional system for identifying the potential significance of diffusive mass-transfer in basin diagenesis; and an example where a reactive water is slowly injected into a siliciclastic system.

3. Water–rock interaction model

Changes in solute species concentrations due to mineral dissolution and precipitation reactions, inter-ionic equilibrium reactions and diffusive and advective mass transport have been previously described in the form of a continuity equation (Ortoleva et al., 1987)

$$\frac{\partial \phi c_\alpha}{\partial t} = D_\alpha \nabla^2 (\phi c_\alpha) - \vec{\nabla} \cdot (\phi c_\alpha \vec{u}) + \sum_{j=1}^{N_a} \omega_j \frac{W_j}{\varepsilon} - \sum_{i=1}^M v_{\alpha i} \rho_i \sum_{\gamma=x,y,z,f,n} A_{\gamma i} G_{\gamma i} \quad (1)$$

for porosity ϕ , α species solute activity c_α and diffusion coefficient D_α , rock flow velocity \vec{u} , N_a number of fast reactions of rate ω_j , solid molar density of the i th mineral ρ_i , stoichiometry of solute α in the i th slow reaction $v_{\alpha i}$, and surface area of i -th mineral $A_{\gamma i}$. Surface area type (free-face, vertical and horizontal grain–grain contact areas) is indicated by the subscript γ , and M number of kinetic reaction rates by $G_{\gamma i}$. Reaction rate W_β depends on pore fluid composition, and the smallness parameter ε explicitly emphasizes that the N_a reactions are fast. In order, the first two terms on the right-hand side of Eq. (1) are diffusive and advective fluxes, respectively, and the latter two terms identify contributions due to equilibrium (fast) reactions in pore water and kinetic (slow, or finite-rate) reactions of minerals, respectively.

Typically, many aqueous reactions are at equilibrium. For carrying out analytical or numerical studies of water–rock systems it is useful to rewrite the reaction–transport equations in such a way that the fast reactions are always at equilibrium, while the full temporal and spatial dynamics of the relatively slow processes is sustained.

First, each chemical reaction is represented as a vector of length N , the number of aqueous species. Then, in the limit as $\varepsilon \rightarrow 0$, Eq. (1) can be reduced to two types of equations (Ortoleva et al., 1987; Ortoleva, 1994). The first set of these two types that preserve the slow-reaction process has the form

$$\xi^{(j)} \left[\frac{\partial \phi c}{\partial t} = -\vec{\nabla} \cdot \vec{J} + \Delta W \right] \quad j = 1, 2, \dots, (N - N_a), \quad (2)$$

where \vec{J} combines both diffusive and advective transport components, Δ is an $N \times M$ matrix of stoichiometric coefficients for the M slow reactions, and W is a column vector of the M rates of the slow reactions. The vectors $\xi^{(j)}$ are orthogonal vectors that satisfy the condition $\xi \cdot \Omega = 0$, where Ω is an $N \times N_a$ stoichiometric matrix for the N_a fast reactions. For a system consisting of N aqueous species and N_a fast reactions there exists exactly $(N - N_a)$ vectors that satisfy the orthogonal condition.

The second type of equations follows from the equilibrium conditions among the solute species:

$$\sum_{\alpha=1}^N v_{\alpha k} \mu_\alpha = 0, \quad k = 1, 2, \dots, N_f, \quad (3)$$

where $v_{\alpha k}$ is the stoichiometry of solute α in the k th equilibrium reaction, and μ_α is the chemical potential of solute α . To obtain the ξ vectors the QR decomposition method (Atkinson, 1988) is used. Further details and generalizations for the treatment of thermodynamically redundant reactions can be found in Ortoleva (1994).

Completing Eqs. (2) and (3) are descriptions of activity of solutes according to the B-dot activity correction method of EQ3/6 (Wolery et al., 1990), and the reaction rate law

$$G_{\gamma i} = k_{i,diss} \left(\prod_{j=1, v_j < 0}^N c_j^{-v_{ij}} - \prod_{j=1, v_j > 0}^N c_j^{v_{ij}} \frac{1}{K_{\gamma i}} \right), \quad (4)$$

where j identifies the aqueous species index, and $k_{i,diss}$ and K_i are dissolution rate constant and equilibrium constant of mineral i for facet γ , respectively. The two product factors are reactant and product species, respectively.

The temperature dependence of rate in Eq. (4) is accounted for by an Arrhenius expression:

$$k_{i,diss} = k_{i,o} \exp\left(\frac{-Ea_i}{RT}\right), \quad (5)$$

where $k_{i,o}$ is the high-temperature limit of dissolution rate constant, Ea_i is the activation energy, and R and T are the gas constant and pore-water absolute temperature, respectively.

The porosity and temperature dependence of the diffusion coefficient is taken to be

$$D_\alpha = D_{\alpha o}^{-\left(\frac{E_{D\alpha}}{RT}\right)} \phi^{2/3}, \quad (6)$$

where $D_{\alpha o}$ is the diffusion coefficient in free-water at room temperature and $E_{D\alpha}$ is the activation energy. The exponential expression $\phi^{2/3}$ accounts for the effect of tortuosity in the porous medium (Bear, 1972). The temperature dependence is based on the work of Krooss and Leythaeuser (1988). Dispersivity is not considered in this study due to low water flow velocities in diagenetic environments.

4. Composite medium model

Complementing the multi-mineralic reaction model is a composite media approach to rock description and evolution. This dynamic texture model allows sediments to be described as porous media consisting of a number of minerals, where each mineral is described by geometric and textural properties, such as grain size, volume, and surface area.

First, total volume of a unit sediment packet is described as

$$\phi = 1 - \phi_i = 1 - \sum_{i=1}^M n_i V_i, \quad (7)$$

where ϕ_i , n_i and V_i are volume fraction (mode), mineral number density (number of mineral grains per unit volume) and granular volume of i th mineral, respectively. Geometries of grains can be chosen to be one of several types (sphere, cylinder, prism, etc.), and granular volume of a mineral can be described by geometric length variables, such as radius, length and height. Consequently, a mineral volume, surface area and mass can be calculated by using these variables, specific gravity, and molar density.

Change in sediment composition resulting from precipitation and dissolution of minerals is computed from mineral reaction rates and surface areas. Mineral-specific textural and geometric descriptions of this textural model allows calculations of surface areas and porosity that are used in Eqs. (2) and (3) to be consistent with the evolving sediment property.

Permeability of sediment is also calculated using the instantaneous, local textural information (e.g., porosity and the grain geometries), using a modified form of Kozeny–Karman equation (Bear, 1972):

$$k = k'(10^{-6}) \left(\frac{\langle L \rangle}{2} \right)^2 \frac{\phi^3}{(1 - \phi)^2}, \quad (8)$$

where k and k' are permeability of the sediment and low-porosity permeability coefficient, respectively. The parameter $\langle L \rangle$ is the mode-normalized tortuosity effect approximated by

$$\langle L \rangle = \sum_{i=1}^M \frac{\phi_i L_i}{(1 - \phi)}, \quad (9)$$

where ϕ_i and L_i are mode and grain diameter of mineral i . The low-porosity permeability coefficient is based on the assumption that permeability decreases exponentially more rapidly, controlled by exponent of ω , when porosity reaches some low threshold value ϕ_{cr}

$$k' = \exp \left\{ \frac{-\phi_{cr}}{\phi} \right\}^{\omega}, \quad (10)$$

where ω is a phenomenological coefficient (taken to be 1.0 in the simulations below).

5. Program organization

Simulator WRIS.TEQ is a subset of a more comprehensive basin- and reservoir-scale simulator CIRF.B that addresses evolutions of stress, fracturing, multi-phase fluid flow, diagenesis and organic matter decomposition (Payne et al., 2000; Tuncay et al., 2000a, b). Up

to 13 partial differential equations (PDEs) are solved by CIRF.B using an iterative forward-time stepping method. A number of modules are installed on CIRF.B, each of which solves one or more PDEs, and/or other phenomenological equations. The core structure of CIRF.B includes an array of data managing interfaces that allow geologic data as well as physical and chemical constants and material properties data to be input. The modular structure of CIRF.B allows independent developments of each module, and also allows selective reconfiguration of modules to produce task-specific simulators. Thus, WRIS.TEQ represents a specific configuration of CIRF.B modules that accounts for fluid flow, water–rock interaction (diagenesis), and texture evolution processes.

The structure of CIRF.B and WRIS.TEQ is shown in Fig. 1. The program manages geological boundary conditions, such as sedimentation and erosion, subsidence, deformation, and fluid flux histories, as distinct from the fundamental data, such as chemical and physical constants and material properties. Whereas the first data type is assembled and input by a user for a site-specific study, the second type of data is maintained in the program library. In the program, both data types are gathered and assimilated in the Initialization Stage shown in Fig. 1. Computation of the designed system is carried out in the Simulator Core segment using controlled time stepping and layered iterations of PDEs and PDE groups.

The iterative solution of the PDEs is necessary to preserve their strong nonlinearity. In addition, groups of PDEs may have uniquely specific sensitivities, that must be resolved before the solutions can be used for other PDEs. Thus, to advance the whole system for one time step, the entire ensemble of the PDEs must be iterated two or more times.

To further aid the solution of the PDEs, an aggressive time-step controlling procedure is implemented in the program. Thus, each time step is estimated at the beginning of the main iteration loop according to the rates of change of several system properties (e.g., mineral dissolution/precipitation, porosity change, fluid pressure change, sedimentation and erosion, subsidence, and temperature change rates). However, if the determined time step is still too large (e.g., one of the modules fails to converge or produces unacceptably large change in a property), the time step is decreased and the iteration is restarted from the beginning. The time step is gradually increased, when the system regularly converges to a stable and consistent solution. For any given simulation, it is typical for the time step to fluctuate between minutes to thousands of years as water–rock interactions progress.

An additional advantage of the modular construction of CIRF.B is the flexibility in the types of numerical methods that can be used to solve the PDEs in each

CIRF.B program structure and WRIS.TEQ components

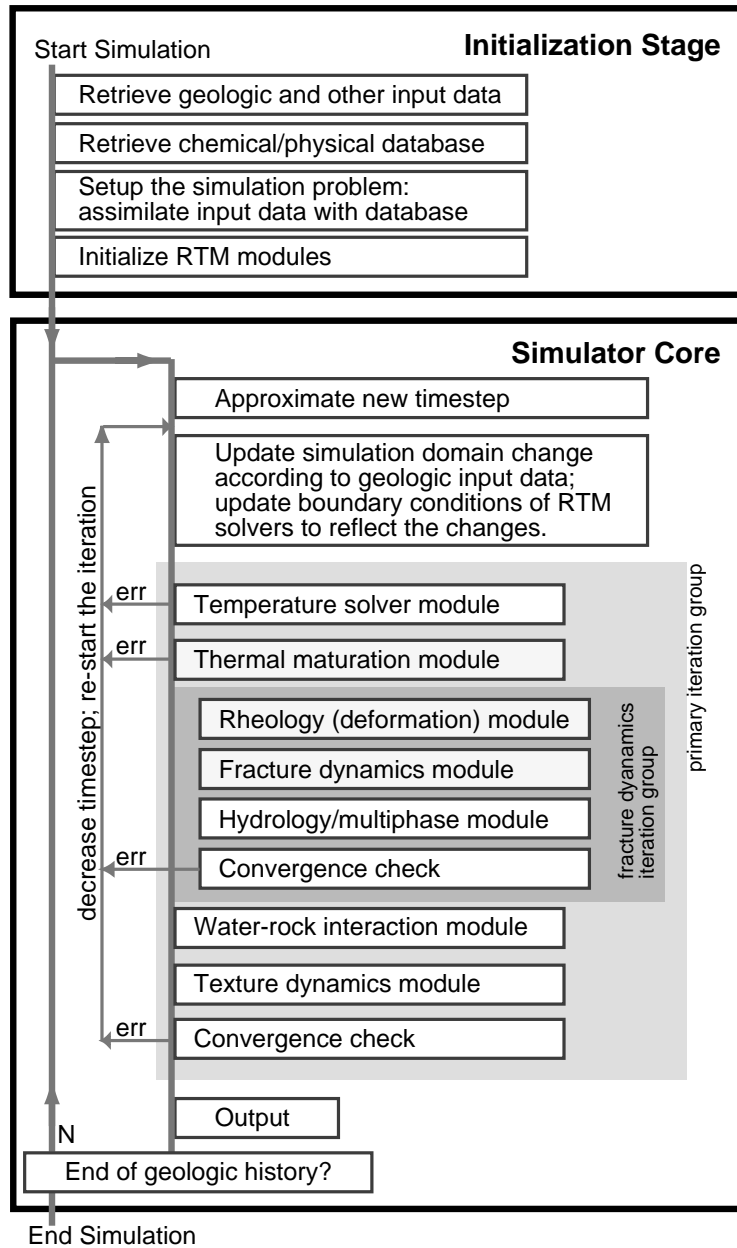


Fig. 1. Shown is flow chart of CIRF.B program, which consists of initialization segment that sets up simulation domain and data, and simulator core that solves partial differential equations (PDEs). Modular installation of PDE modules in CIRF.B allows program to be configured for variety of geological problems. WRIS.TEQ program uses hydrology, water–rock interaction and textural dynamics modules. Thermal maturation, rheology and fracture dynamics modules are not used in WRIS.TEQ.

module. All modules are based on one- to three-dimensional arrays of hexahedral finite elements, where the solution of the system is solved globally. The exceptions are the water–rock interaction module and the textural module, which are based on point-solvers, i.e., each element is solved locally, but iterated globally.

In the water–rock interaction module, the mass-transfer is resolved by iterating the point solver with an advective and diffusive transport discretization function (Fig. 2). Fluid flow is computed in the multiphase solver. Convergence is achieved when the successive iteration produces insignificant correction to

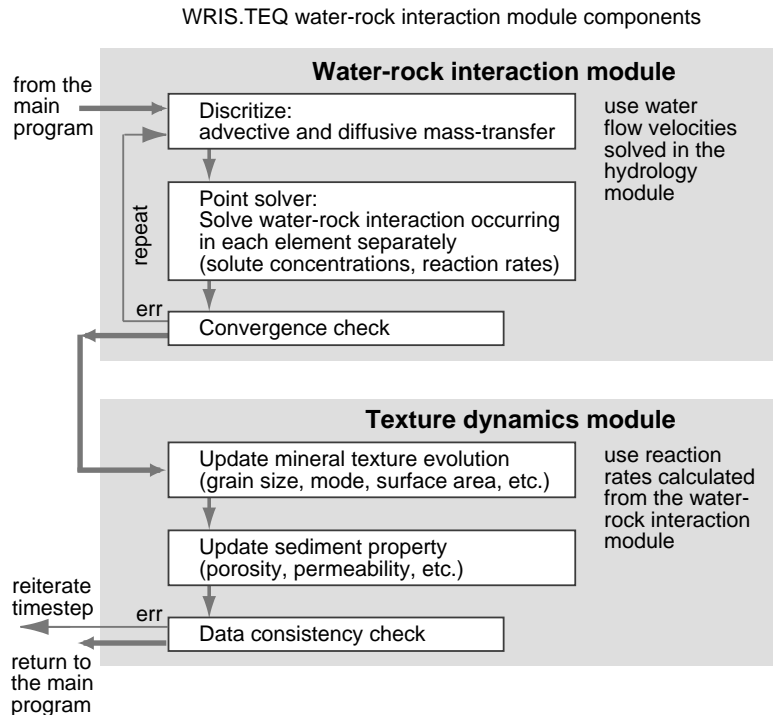


Fig. 2. Water–rock interaction textural dynamics modules of CIRF.B are core components of WRIS.TEQ program. Water-flow vectors from hydrology module is discretized prior to invoking water–rock interaction (point) solver for each element of simulation domain. Nonlinear feedback due to diffusive and advective mass-transfer and water–rock interaction is captured by iterating this discretization–point solver couple until consistency in results are attained. Subsequently, texture dynamics module evolves sediment property using reaction rates calculated from point solver. Global data consistency check is also carried out in latter module. If texture evolution is too rapid, or if convergence is not attained, time step is re-iterated from beginning using smaller value.

pore-water compositions. In the textural module geometric properties are modified according to the reaction rates calculated by the water–rock interaction module.

6. Numerical methods

Each module of CIRF.B uses its own unique numerical methods. The modules that solve rheology, fluid flow and temperature use finite-element methods with various pre-conditioners and matrix solvers. Details of the phenomenology and numerical methods used to solve them can be found in other articles (Tuncay et al., 2000a, b).

The point solver in the water–rock interaction module solves Eqs. (2)–(4) using an iterated Newton–Raphson method (Atkinson, 1988). The mass-transfer terms are discretized in the function external to the point solver. For the discretization, total flux into and out of each element provided by the multiphase module is recalculated as flow vectors by dividing the fluxes by the element surface areas. To allow the use of finite difference-style discretization of the transport terms, the simulation domain of WRIS.TEQ is constrained to

be rectilinear, but not necessarily regular. “Up-winding” is used when discretizing.

Within the point solver, reaction rates, equilibrium constants, the ionic strength of the pore water and the activity coefficients of solutes are computed at the beginning of each Newton–Raphson iteration. The solution is obtained by using the full-pivoting Gauss–Jordan reduction method (Atkinson, 1988), or LU decomposition (Press, 1992). Tests show that both methods achieve identical results, however the LU decomposition method appears to be 5–10% faster.

Even with LU decomposition, obtaining the solution can be difficult due to large differences in solute concentrations, which results in badly conditioned Jacobians. Therefore, to further enhance the numerical solution method, Eqs. (2)–(4) are rewritten to use the variable x_i using the transform

$$c_i = e^{x_i}. \quad (11)$$

As a result, the Newton–Raphson method is used to solve for x_i , which is translated back to c_i upon completion of each iteration.

In the textural dynamics module, geometric properties of the minerals are calculated using a simple explicit

forward-difference method using the reaction rates obtained from the water–rock interaction module and previous time step mineral properties. For simple geometric shapes, exact volumes of minerals precipitating or dissolving are calculated using the mineral reaction rates, surface areas, specific volumes, molar densities, and the time step. Porosity is recalculated once the individual mineral volume fractions are modified; permeability is then calculated using the porosity and the modified grain geometric data.

Iteration of the fluid-flow computation, water–rock interaction, and texture modification are repeated two or more times for any given time step to capture the nonlinearity among the water–rock interaction, texture dynamics, and fluid flow. A time step is determined to be complete when pore water composition and textural parameters converge to a stable solution.

In addition to a convergence test, the program also checks for inconsistent or unacceptably large changes in any of the sediment properties before starting the next time step. For instance, if porosity or the mode of any mineral anywhere in the system changes more than 0.2%, the computation is re-started with a smaller time step.

7. Compositional disequilibrium

Compositional disequilibrium in multi-mineralic porous media can occur when one or more of the minerals are composed of common constituents, but have distinct chemical and physical properties. Thus, sediments that are composed of many minerals are chemically unstable, so that one or more minerals will tend to dissolve and favor the precipitation of others. The rate of this process depends on reaction mechanisms of minerals, and whether the solute is being replenished through either advective or diffusive mass-transfer.

A simple example of compositional disequilibrium-driven water–rock interaction is the precipitation of higher order crystalline quartz from lower-order opal and chalcedony (Ozkan and Ortoleva, 2000). In this example opal is thermodynamically less stable than quartz; the speed at which this transformation can occur depends on temperature and whether there is an external source of additional silica.

A more complex example of composition-driven sediment diagenesis is the precipitation of muscovite in the system quartz–K-feldspar–muscovite–kaolinite (see Fig. 3). Initial conditions, including the volume fractions, grain size, reaction rate parameters, and temperature history used for the simulation are shown in Tables 1 and 2. All minerals are assumed to retain spherical grain geometry throughout the simulation. The simulation was run in a batch mode that uses a single numerical element with no flux into or out of the system.

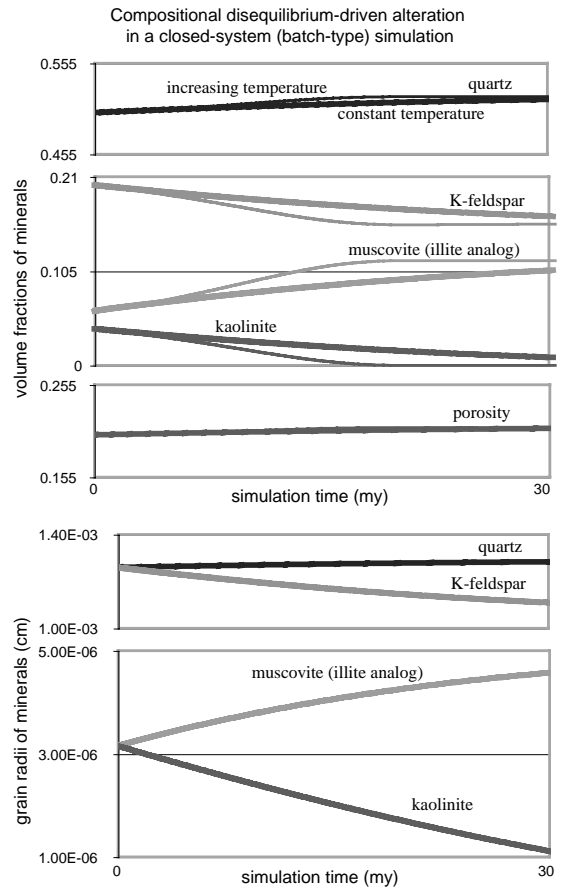


Fig. 3. WRIS.TEQ simulation of batch-type closed system consisting of quartz, K-feldspar, muscovite (illite analog), and kaolinite is shown. Tables 1 and 2 list conditions used for this simulation. Stable mineral assemblage of system is quartz, K-feldspar, and muscovite; any amount of kaolinite present will dissolve to form muscovite and quartz. Dissolution of K-feldspar is due to depleting potassium in water. Increasing temperature increases reaction rates (thin lines). Slight curvatures in volume fraction profiles are due to changing grain sizes and surface areas of minerals with progressing reactions.

Thus, all changes in the sediment compositions and properties are due to reactions that are driven by the compositional disequilibrium among the minerals. The stable assemblage of this system is quartz–K-feldspar–muscovite, such that any kaolinite present will result in precipitation of muscovite and quartz at the expense of K-feldspar and kaolinite.

Temperature is an important physical condition that strongly affects water–rock interaction. A second simulation was carried out for the identical system, but subject to a linear increase of 4°C per million years. Increases in mineral solubilities, as well as rate constants, result in effective increases in mineral transformation rates. For both examples, slight

Table 1
Equilibrium constants of reactions are from EQ3/6 database (Wolery, 1992)

Mineral	Reaction stoichiometry	Rate constant	Activation energy	Adjust factor
<i>Slow reactions (kinetic mineral dissolution reactions)</i>				
Quartz	$\text{SiO}_2 = \text{SiO}_{2(\text{aq})}$	0.041719	91410	0.005
K-feldspar	$\text{KAlSi}_3\text{O}_8 + 2\text{H}_2\text{O}$ $= \text{K}^+ + \text{Al}(\text{OH})_3 + 3\text{SiO}_{2(\text{aq})} + \text{OH}^-$	1.59283E-06	56520	0.005
Anorthite	$\text{CaAl}_2\text{Si}_2\text{O}_8 + 4\text{H}_2\text{O}$ $= \text{Ca}^{2+} + 2\text{Al}(\text{OH})_3 + 2\text{SiO}_{2(\text{aq})} + 2\text{OH}^-$	1.26555E-06	56520	0.005
Albite	$\text{NaAlSi}_3\text{O}_8 + 2\text{H}_2\text{O}$ $= \text{Na}^+ + \text{Al}(\text{OH})_3 + 3\text{SiO}_{2(\text{aq})} + \text{OH}^-$	1.00721E-06	56520	0.005
Muscovite	$\text{KAl}_3\text{Si}_3\text{O}_8 + 4\text{H}_2\text{O}$ $= \text{K}^+ + 3\text{Al}(\text{OH})_3 + 3\text{SiO}_{2(\text{aq})} + \text{OH}^-$	1.0736E-12	30430	0.005
Kaolinite	$\text{Al}_2\text{Si}_2\text{O}_7 \cdot 2\text{H}_2\text{O} + \text{H}_2\text{O}$ $= 2\text{Al}(\text{OH})_3 + 2\text{SiO}_{2(\text{aq})}$	1.36482E-12	30430	0.005
Calcite	$\text{CaCO}_3 = \text{Ca}^{2+} + \text{CO}_3^{2-}$	1.79126E-19	25790	0.0001
<i>Primary solute</i>				
Reaction stoichiometry				
<i>Fast reaction (equilibrium reactions among solutes)</i>				
H_2O	$\text{H}_2\text{O} = \text{H}^+ + \text{OH}^-$			
CO_3^{2-}	$\text{HCO}_3^- = \text{H}^+ + \text{CO}_3^{2-}$			
HCO_3^-	$\text{H}_2\text{CO}_3 = \text{H}^+ + \text{HCO}_3^-$			

Rate constants and activation energy are from a variety of sources, and calculated from published experimental results. Unit of rate constant and activation energy are cm/s and K-joules/mole, respectively. Adjustment factors are used to calibrate experiment-derived data to observed rate behavior of sediments in basins using WRIS.TEQ.

Table 2
Sediment composition and conditions used for simulation of Fig. 3

Mineral	Mode	Grain radii (cm)	Simulation conditions
Quartz	0.5	0.01	Temperature: simulation 1 simulation 2 (linear increase of 4°/my) Simulation duration Number of elements used Mass-transport
K-feldspar	0.2	0.01	
Muscovite	0.06	0.0005	
Kaolinite	0.04	0.0005	
			80°C
			80–203°C
			30 my
			1 (batch-type)
			closed-system

Albite, anorthite and calcite were not included.

curvatures evident in volume-fraction profiles with time result from changing mineral grain sizes and surface areas.

8. Spatial relations in a diffusion-dominated system

An important facet of water–rock interaction is that only a small amount of mineral is required to change the concentrations of solutes in water significantly. Conversely, significant volumes of water are required to create small changes in mineral composition. Thus, to explain the observed extensive diagenetic alterations of sediments, it has been necessary to invoke complex

scenarios that require unreasonable amounts of water to flow through sediment.

However, mass transfer between sediments can occur through both advection and diffusion. Diffusion is a mechanism whereby solutes migrate through water, from a higher-concentration region to a lower-concentration one, even if the water is not moving. A crude approximation assuming the typical diffusion coefficient of $5.0 \times 10^{-6} \text{ cm}^2/\text{s}$ suggests that solutes can migrate as much as 5 cm/year in sediment with 30% porosity (Park and Ortoleva, 1998). Thus, for many basins, diffusive mass-transfer is a viable mechanism whereby significant mass can be moved over geologic time (Thyne, 2001).

Both advective and diffusive mechanisms are strongly affected by porosity and pore connectivity. For a diffusion mechanism to be effective two conditions must be met: (1) concentration gradients must persist in sediments; and (2) sufficient time must be available for the slow diffusion process to produce significant cumulative mass-transfer. In geologic environments the first condition is easily met when sediments are compositionally and texturally heterogeneous. Secondly, because each sediment volume tends toward establishing its own unique solute composition, any two adjacent

sediment volumes with different compositions and textures can establish solute-concentration gradients.

Shown in Fig. 4 are the results of a simulation that demonstrates the effectiveness of diffusive transport as a process in sediment diagenesis. As documented on Table 3, four sediment layers of varying composition and thickness were arranged vertically (Fig. 4A). Simulation was started at 1500 m depth, and subsided at a constant rate of 120 m/my. Given the geothermal gradient of 32°/Km, this is equivalent to increasing the sediment temperature at a rate of 3.84°/my. The system

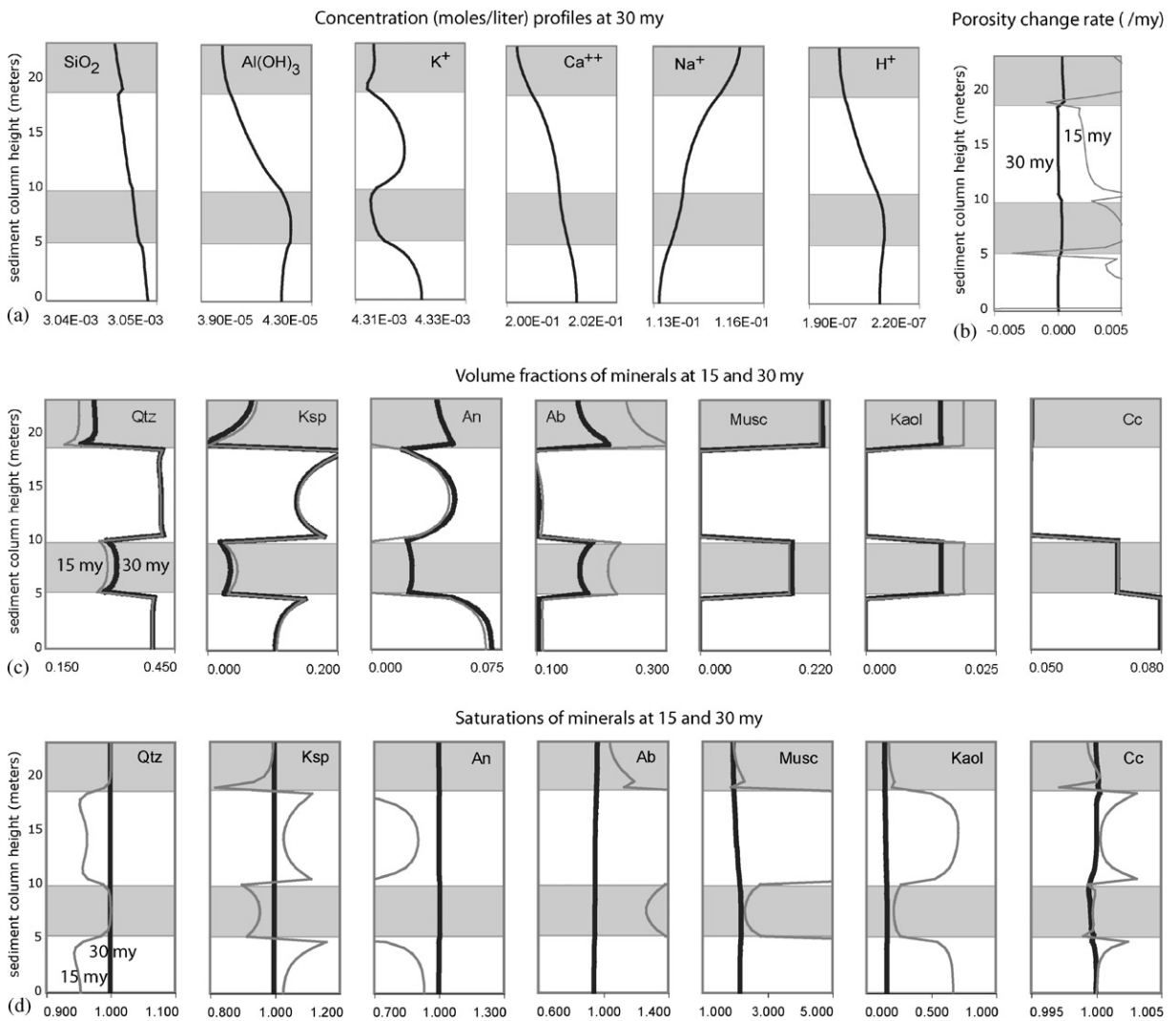


Fig. 4. WRIS.TEQ simulation of heterogeneous sediment column consisting of 7 minerals; (A) solute concentration profiles, (B) instantaneous porosity change rate, (C) mineral volume fractions, and (D) saturations of minerals, are shown. Results are after 30 my of simulated geologic time. (B) Also show volume fractions at 15 my (thin lines). Descriptions of lithologies and conditions used for simulation are given on Table 2. To test potential significance of diffusive mass-transfer coupled with composition disequilibrium-driven reactions, no water was injected. These profiles demonstrate compositional disequilibrium within each sediment type, diffusion of solutes, and finite reaction rates of minerals strongly interact to enhance original sedimentologic heterogeneity.

Table 3

Sediment column configuration and other properties used for one-dimensional diffusive mass-transfer dominated simulation of Fig. 4

Lithology	Thickness (m)	Number of elements	Simulation conditions				
1. Shale	5.0	10	Starting depth		1500 m		
2. Sand A	8.0	16	Subsidence rate		120 m/my		
3. Silt	5.0	10	Geothermal gradient		32°/Km		
4. Sand B	5.0	10	Temperature range 80 (start)–163.2°C (end)				

Lithology	qtz	kspar	an	ab	musc	kaol	cc
<i>Volume fractions of minerals</i>							
1. Shale	0.3	0.1	0.08	0.06	0.2	0.02	0.05
2. Sand A	0.45	0.12	0.08	0.06	0	0	0.05
3. Silt	0.35	0.08	0.06	0.06	0.15	0.02	0.07
4. Sand B	0.42	0.1	0.09	0.07	0	0	0.08
<i>Grain radii (mm) of minerals</i>							
1. Shale	0.005	0.005	0.005	0.005	0.0005	0.0005	0.02
2. Sand A	0.05	0.04	0.04	0.04	0.0005	0.0005	0.05
3. Silt	0.01	0.01	0.01	0.01	0.0005	0.0005	0.02
4. Sand B	0.08	0.05	0.05	0.05	0.0005	0.0005	0.04

was closed to influx of water from outside, i.e., water was not injected into the system. Four types of variables are presented in Fig. 4: volume fractions and saturations of minerals, porosity change rates, and concentration profiles of select solute species.

Several interesting observations can be made. Most notably, minerals can either dissolve or precipitate over geologic time in the absence of significant fluid flow. Solute concentration profiles indicate that chemical gradients exist across the sediment layers. Mineralization patterns across the sediment boundaries are more pronounced compared to the mid-regions, further demonstrating that compositional differences across sediment layers, and flux of solutes resulting from it, are responsible for the enhancement of the local heterogeneity.

Concentration and saturation profiles provide even more insight into the mechanism of diffusive transport and mineral precipitation/dissolution patterns. Strong dependence of aluminum concentration on clay reactivity is here demonstrated by closely matching aluminum concentration and muscovite saturation profiles. The potassium concentration profile exhibits a more complex spatial pattern, and correlates somewhat with the K-feldspar saturation profile. Also, calcite is dissolving in the lower silt unit but precipitating along the margin of the upper shale. Likewise, solutes and saturations of other solutes and minerals can be correlated to varying degrees, reflecting complex interrelations of concentration, composition, texture and thermal profiles.

Overall, in this system consisting of seven of the most common diagenetic minerals, the compositional and textural differences between the sediment layers cause

extensive diagenetic alteration in over the scale of geologic time.

9. Spatial relations in an advection-dominated system

An example of advective mass-transfer induced localized alteration of sediments is presented in this section. This example is a continuous simulation of the system shown in Fig. 4 and Table 3, but, after 30 my, an externally derived volume of water is injected into the system from the bottom at a fixed flux of 0.8 cm/yr for the duration of 1 my. Given the sediment porosity of 20% this flux rate produces 4 cm/yr fluid flow velocity. The composition of the injected water was derived by letting the simulation of Fig. 4 to reach 31 my; the composition of the water from the lower-most sediment packet (Table 4) was recorded, and used in this advective system simulation.

Changes in concentration and saturation at various times are shown in Figs. 5A and B, respectively, from the onset of fluid injection until the time at which the concentration profiles establish near steady-state patterns. Saturations, mineral volume fractions, porosity and porosity change rates at 30 and 31 my are shown in Figs. 6A–D, respectively.

Concentration profiles of Fig. 5A show that higher-concentration solutes, such as Ca^{++} and Na^{++} , eventually establish profiles reflecting the inlet concentrations, whereas lesser-concentrated solutes, such as K^+ , SiO_2 , $\text{Al}(\text{OH})_3$, and H^+ , show more strong variability with lithology. Saturation profiles (Fig. 5B)

Table 4
Composition and saturation of invasive water used for simulation of Figs. 5 and 6

Species	(mol/l)	Species	(mol/l)
Composition of invasive water			
SiO ₂	0.00326	H ⁺	2.51(10 ⁻⁷)
Al(OH) ₃	3.722(10 ⁻⁵)	K ⁺	0.00507
Ca ⁺⁺	0.195	Na ⁺	0.125
CO ₂ (CO _{2(aq)} + HCO ₃ ⁻ + H ₂ CO ₃)	2.145		
Mineral	Saturation	Mineral	Saturation
<i>Saturation of invasive water (at 170°C)</i>			
Quartz	1.0	K-feldspar	0.999
Anorthite	1.0	Albite	0.953
Muscovite	2.18	Kaolinite	0.125
Calcite	1.0		

Water composition was derived by letting simulation of Fig. 4 continue to 31 my; composition is from lower-most point of sediment column.

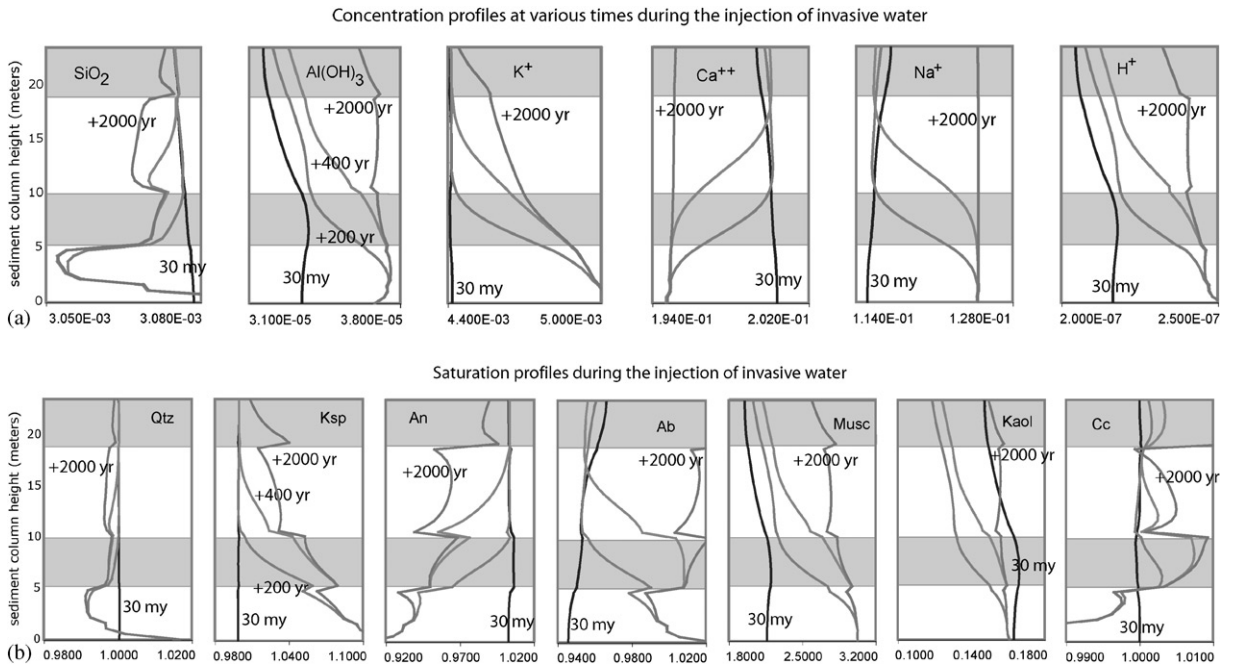


Fig. 5. Advection-dominated system simulation. This simulation is continuation of simulation of Fig. 4, with externally derived invasive water (Table 4) imposed at bottom of column to produce 4–5 cm/yr flow velocity. Concentration profiles (A) and saturations (B) at 30my, +200, +400, and +2000 years are shown. Because concentrations of solutes change according to composition and texture of sediment and property of water, predicting trends of mineralizations far from injection point is difficult without a quantitative, process-oriented model.

show that solute concentrations changes are dramatic as the water passes through each lithology.

Mineral saturations at 31 my (Fig. 6A) show the near steady-state concentration profiles established in the sediment column. Between 30 and 30.4my saturation patterns shift unpredictably (Fig 5B), but show consistent lithologic dependence. Net changes in mineral

volume fractions (Fig. 6B) show that the most significant changes occur near the inlet. Porosity (Fig. 6C) and the rate of porosity change (Fig. 6D) at 31 my show that sandstones are reacting less than shales. However, the upper shale shows a significantly higher rate of change than the lower shale. Rates of Porosity change are also greater along lithologic boundaries.

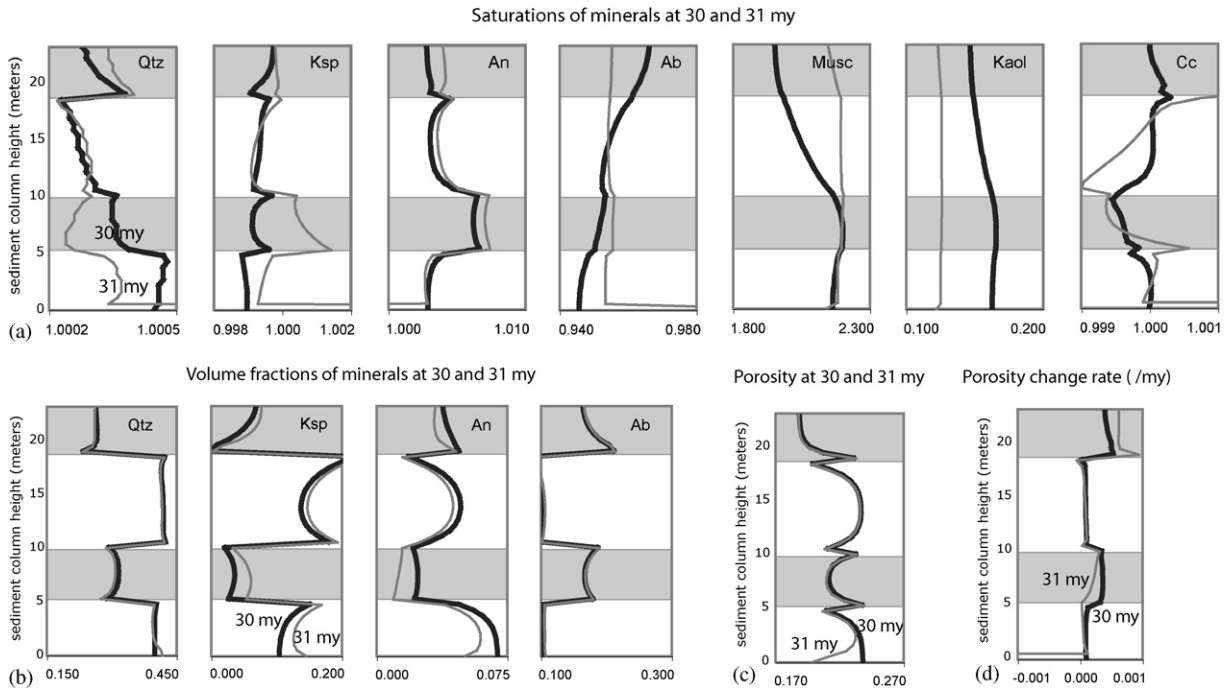


Fig. 6. Comparison of various properties; (A) saturations and (B) volume fractions of minerals, (C) porosity, and (D) instantaneous porosity change rate (/my) at 30 and 31 my are shown. Kaolinite, muscovite and calcite showed little change in volume fractions, and not included in (B). Flow rate in sediment column varies from 4 to 5 cm/yr depending on porosity. Most extensive porosity change occurs near inlet point. Lithologic dependence of solute concentration profiles is also clearly evident.

A number of simplifying assumptions were used in the simulations shown in Figs. 5 and 6. For instance, only seven major diagenetic minerals were used to characterize the lithologies, and the two-dimensionality of flow in stratified lithologies was ignored. Most significantly, invasive water was let into the system for one million years continuously at a high rate of flux. Nonetheless, the simulation demonstrates that advection-driven diagenesis can produce highly variable alteration patterns that depend on sediment composition, texture, and the composition of invasive water. It is reasonable to expect that changing any one of these conditions would produce different mineralization patterns than those shown in Figs. 5 and 6.

10. Discussion

A significant limitation of diagenetic models has been that they do not account for the effects of all the important basin-scale processes, including mechanical compaction, deformation, hydrocarbon generation and basin-scale multiphase flow. Although such a simulator was not possible in the past, due to limitations of older computers, the recent advances in computing platforms and increasing acceptance of quantitative and process-

oriented models in geology are now making comprehensive simulators possible. Thus, coupling a diagenetic model in the framework of a process-oriented basin model is an important step forward, and the advances WRIS.TEQ and CIRF.B represent an ambitious attempt to accomplish this goal.

The two simulation examples presented in this article identify the importance of both diffusive and advective mass transfer in diagenetic environments. Diffusive mass transfer is a pervasive, long-term process that affects sediments throughout a basin, but most significantly for systems that are highly heterogeneous in composition and texture; advective mass transfer is a short-lived process that can significantly affect local sediment alteration. Whereas the effects of the diffusive process can be predicted given a stratigraphy with detailed facies or compositional data, subsidence and thermal histories, assessing the effects of advective transport requires a more detailed knowledge of sediments and basin history to provide detailed water migration histories.

Results on the advective mass-transfer-dominated system show that diagenesis involving appreciable fluid flow is inherently a strongly coupled process between flow and texture evolution. Thus, while only one-dimensional systems are presented in this article,

regional and site-specific studies are best accomplished by accounting for full 2-dimensionality of the system.

The phenomenology presented in this paper can be further extended to include factors such as higher ionic strength corrections (e.g., Pitzer-correction (Pitzer, 1987)), sorption isotherms (Haworth, 1990), colloid and microbial activity (Domenico and Schwartz, 1998), dispersion (Boudreau, 1996), more complex grain shape and surface texture descriptions, unsaturated flow, and worm-holing/karsting (Ormond and Ortoleva, 2000). These additional processes would further improve the model predictions, and will allow the program to be used in near-surface environmental as well as other water–rock interaction problems, such as CO₂ sequestration.

11. Conclusion

Sediments can be characterized as compositionally unstable complex reactive porous media. Thus, water–rock interactions are driven by the state of disequilibrium that persists in sediments. Inherently, therefore, water–rock interaction processes are multi-mineralic and kinetic.

WRIS.TEQ is a problem-specific simulator that is configured by using select modules of CIRF.B. It is designed to simulate water–rock interactions in heterogeneous porous media, and accounts for kinetic and thermodynamic reactions among solids and solutes, texture evolution, and the nonlinear coupling of these processes with fluid flow. It is designed specifically to address the issues of composition, and advective and diffusive mass-transfer on sediment alteration.

Significant alteration of sediments can occur in situations where a large flux of water occurs. In sedimentary basins, however, it is usually difficult to account for sufficient water to account for the extensive diagenetic alterations observed. Thus, in this situation, slow but persistent diffusive mass-transfer becomes important. WRIS.TEQ simulation examples show that: (1) compositional disequilibrium is sufficient to make significant textural change in geologic time; (2) the same water–rock interaction process also creates conditions where significant mass-transfer can occur over tens of meters in geologic time; and (3) advective mass transport can produce localized alteration of sediment composition and texture: however, its effectiveness depends strongly on the composition and availability of invasive water.

Acknowledgements

This study was supported in part by the US Department of Energy, Office of Basic Energy Sciences,

under grant no. DE-FG02-91ER14175 A010. The authors benefited from discussions with Geoff Thyne. Comments from the anonymous reviewers contributed to the quality of this manuscript. Also, patience and diligence of Lauren Browning is very much appreciated.

References

- Atkinson, K., 1988. *An Introduction to Numerical Analysis*. Wiley, New York, NY, 693pp.
- Bear, J., 1972. *Dynamics of Fluids in Porous Media*. Elsevier, New York, NY, 764pp.
- Boudreau, B., 1996. *Diagenetic Models and their Implementation*. Springer, New York, 414pp.
- Chen, W., Ghaith, A., Park, A., Ortoleva, P., 1990. Diagenesis through coupled processes: modeling approach, self-organization, and implications for exploration. In: Meshri, I., Ortoleva, P. (Eds.), *Prediction of Reservoir Quality through Chemical Modeling*. American Association of Petroleum Geologists Memoir 49, pp. 103–130.
- DeGroot, A., Mazur, P., 1962. *Non-equilibrium Thermodynamics*. North-Holland Publishing Co., Amsterdam, The Netherlands, 510pp.
- Domenico, P., Schwartz, F., 1998. *Physical and Chemical Hydrogeology*, 2nd edition. Wiley, New York, NY, 506pp.
- Garrels, R., Christ, C., 1990. *Solutions, Minerals, and Equilibria*. Jones and Bartlett, Boston, MA, 450pp.
- Haworth, A., 1990. A review of the modeling of sorption from aqueous solution. *Advances in Colloid and Interface Science* 32, 43–78.
- Krooss, B., Leythaeuser, D., 1988. Experimental measurements of the diffusion parameters of light hydrocarbons in water-saturated sedimentary rocks. II. Results and geochemical significance. *Organic Geochemistry* 12, 91–108.
- Lichtner, P., 1985. Continuum model for simultaneous chemical reactions and mass transport in hydrothermal systems. *Geochimical Cosmochimica Acta* 49, 779–800.
- Ormond, A., Ortoleva, P., 2000. Numerical modeling of reaction-induced cavities in a porous rock. *Journal of Geophysical Research, B, Solid Earth and Planets* 105 (7), 16737–16747.
- Ortoleva, P., 1994. *Geochemical Self-organization*. Oxford University Press, New York, NY, 411pp.
- Ortoleva, P., Merino, E., Moore, C., Chadam, J., 1987. *Geochemical self-organization I: reaction-transport feedbacks and modeling approach*. *American Journal of Science* 287, 979–1007.
- Ozkan, G., Ortoleva, P., 2000. A mesoscopic model of nucleation and Ostwald ripening/stepping: application to the silica polymorph system. *Journal of Chemical Physics* 112, 10510–10525.
- Park, A., Ortoleva, P., 1998. Enhanced heterogeneity and layered mineralization along lithology boundaries: reaction–transport simulation. *American Association of Petroleum Geologists Annual Meeting Extended Abstracts 2*, Salt Lake City, Utah, US, p. A509.
- Parkhurst, D., Thorstensen, D., Plummer, L., 1990. PHREEQE-A computer program for geochemical

- calculations. US Geological Survey Water Resources Investigations Report 80–96, Washington, DC, 193pp.
- Payne, D., Tuncay, K., Park, A., Comer, J., Ortoleva, P., 2000. A reaction-transport-mechanical approach to modeling the interrelationships between gas generation, overpressuring, and fracturing—implications for the Upper Cretaceous natural gas reservoirs of the Piceance Basin, Colorado. *American Association of Petroleum Geologists Bulletin* 84, 545–565.
- Perkins, E.H., Kharaka, Y.K., Gunter, W.D., DeBraal, J.D., 1988. Geochemical modeling of water–rock interactions using SOLMINEQ.88. In: *Proceedings of the American Chemical Society National Meeting* 196, p.GEOC 25.
- Pitzer, K., 1987. A thermodynamic model for aqueous solutions of liquid-like density. In Carmichael, I., Eugster, H. (Eds.), *Reviews in Mineralogy*, vol. 17, Mineralogical Society of America, Washington, D.C. US. pp. 97–142.
- Press, W., 1992. *Numerical Recipes in C: the Art of Scientific Computing*, 2nd edition. Cambridge University Press, Cambridge, UK, 994pp.
- Schechter, R., Bryant, S., Lake, L., 1987. Isotherm-free chromatography: propagation of precipitation-dissolution waves. *Chemical Engineering Communication* 58, 353–376.
- Steeffel, C., Lasaga, A., 1994. A coupled model for transport of multiple chemical species and kinetic precipitation/dissolution reactions with application to reactive flow in single phase hydrothermal systems. *American Journal of Science* 294, 529–592.
- Steeffel, C., Lichtner, P., 1998. Multicomponent reactive transport in discrete fractures: I. Controls on reaction front geometry. *Journal of Hydrology* 209, 186–199.
- Thyne, G., 2001. A model for diagenetic mass transfer between adjacent sandstone and shale. *Journal of Marine and Petroleum Geology* 18, 743–755.
- Tuncay, K., Park, A., Ortoleva, P., 2000a. A forward model of three-dimensional fracture orientation and characteristics. *Journal of Geophysical Research* 105 (B7), 16719–16735.
- Tuncay, K., Park, A., Ortoleva, P., 2000b. Sedimentary basin deformation: an incremental stress rheology approach. *Tectonophysics* 323, 77–104.
- White, A., Chuma, N., 1986. An EQ3/EQ6 reaction path model of chemical evolution in the Valles hydrothermal system, New Mexico, USA. In: Hitchon, B. (Ed.), *Fifth International Symposium on Water–rock Interaction*, Reykjavik, Iceland, pp. 626–628.
- Wolery, T., Jackson, K., Bourcier, W., Bruton, C., Viani, C., Knauss, K., Delany, J., 1990. Current status of the EQ3/6 software package for geochemical modeling. In: *American Chemical Society Symposium Series*, Vol. 416, American Chemical Society, Washington, DC, pp. 104–116.